

Rafiu King Raji,
Xuhong Miao*,
Shu Zhang,
Yutian Li,
Ailan Wan

Influence of Rib Structure and Elastic Yarn Type Variations on Textile Piezoresistive Strain Sensor Characteristics

DOI: 10.5604/01.3001.0012.2527

Ministry of Education,
Jiangnan University,
Engineering Research Center
of Knitting Technology,
Wuxi, P.R. China
* e-mail: miaoxuhong@163.com
e-mail: mrkingraji@outlook.com
e-mail: sheyu880@163.com
e-mail: 327386771@qq.com
e-mail: ailanwan@163.com

Abstract

Production parameters have been established to play a fundamental role in dictating the physical characteristics and sensing properties of knitted sensors. This research studied the influence of elastic yarn type and rib fabric structure variation on the physical, tensile and conductive properties and sensitivity performance of knitted underwear strain sensors to be used for breathing mensuration. Four different structures in 1×1 , 1×2 , 1×3 and 2×2 mock ribs were knitted using covered elastic (CY) and bare strand elastic yarn (BS) combinations. These two parameters proffered unique physical, conductive and tensile characteristics to the samples. Wear and machine tests were conducted to ascertain the sensor's piezoresistive responses. The machine test showed a higher piezoresistive response, with an average peak value (APV) from 1.70Ω to 0.24Ω , while those for the wear test recorded were around 0.0110Ω to 1.867Ω for all sample categories. However, sensors knitted with covered elastic yarns produced the best breathing test results (APV of $1.089 \Omega - 1.86 \Omega$) compared to bare strand elastic yarns (APV $0.0027 \Omega - 0.0790 \Omega$) when used in a wearable environment. Fabric structure variation had influences on both conductive and tensile characteristics; however, the effects on the piezoresistive response were negligible. The influences of the unique characteristics provided by these core parameters on sensor resistance values, piezoresistance, aging, ease of deformation and dimensional stability have also been discussed.

Key words: strain sensor, sensitivity, piezoresistance, elastic yarn, weft knitting.

Introduction

The increased interest in smart clothing as part of the "smart everything" craze has spurred on research into feasible technologies that can afford truly soft and inherent embedment of smart functionality into apparels. Strain sensing, a feasible means of inherently embedding sensors into textile, has been reported in numerous studies with prototype fabrications for motion detection [1], cadence, breathing monitoring [2], etc. Strain sensing in smart textiles is currently based on several technologies including piezoelectricity [3], optical diffraction or interferometry [4], capacitance [5] and piezoresistance [6] impedance [7], piezotronics [8] and photoelastic [9] strain sensing. Also several strain sensors have been fabricated using techniques such as printing, embroidery, over-locking, coating, weaving and knitting. These strain sensors were produced by integrating sensitive or conductive yarns within a non-conductive fabric structure. Several conductive yarns produced via different routes [10] are being experimented on. Even though other forms of textile techniques and

technologies have been used in fabricating textile-based strain sensors, the overwhelming majority of strain sensors sited in literature are weft knitted and mostly produced on flat knitting machines [6, 11, 12]. Knitted strain sensors have found favour in most researches due to the superior flexibility of knitted goods and the comparative suitability of sensitive yarns to the knitting process as opposed to other methods such as weaving [13]. However, regardless of the machine type or yarn types used in sensor fabrication, the two most important requirements of a good strain sensor are sound tensile recovery and high sensitivity response. These properties can be dictated by a number of factors including yarn type, structure type and even machine type [14]. Therefore this study sought to find out as to what extent these parameters affect circular machine knitted strain sensors in terms of their sensitivity and recovery and what optimum parameter is appropriate for good sensor sensitivity.

In Oguzr Atalay's study [12], the impact of design parameters on sensing properties was established, in which a sample was produced on a flat knitting machine. The focus was on the influence of yarn input tension, the number of conductive courses in the sensing structure, and on the elastomeric yarn extension characteristics. Other researches include that of Erhmann *et al* [6], which compared the

suitability of double face, single face, Milano rib and full cardigan knitted on a Stoll CMS-302 TC flat knitting machine for strain sensors. Their studies, however, were not directly focused on a specific application, which renders the setting of the parameters rather vague, as they only suit certain optimum parameters.

This study utilised one of the popular seamless apparel knitting machines widely used for producing intimate apparel – Santoni's SM8 Top2 seamless garment knitting machine. Even though Xie *et al* [15] utilised the same SM8 Top2 machine, their study dealt with the effect of conductive loop arrangements in a plain knit structure unit and its effect on the sensor's sensitivity and repeatability.

So far no study has ever compared the influence of elastic yarn type on strain sensor sensitivity, even though the influence of elastic yarn type on other important fabric performance characteristics exists in literature [16]. Also there has also not been any study on this subject that compared machine sensitivity tests with human wear sensitivity tests. However, the research presented herein gives an indication that there is a good correlation between the two test methods. Moreover in the absence of human volunteers, experiments can be carried out in a lab setting or vice versa.

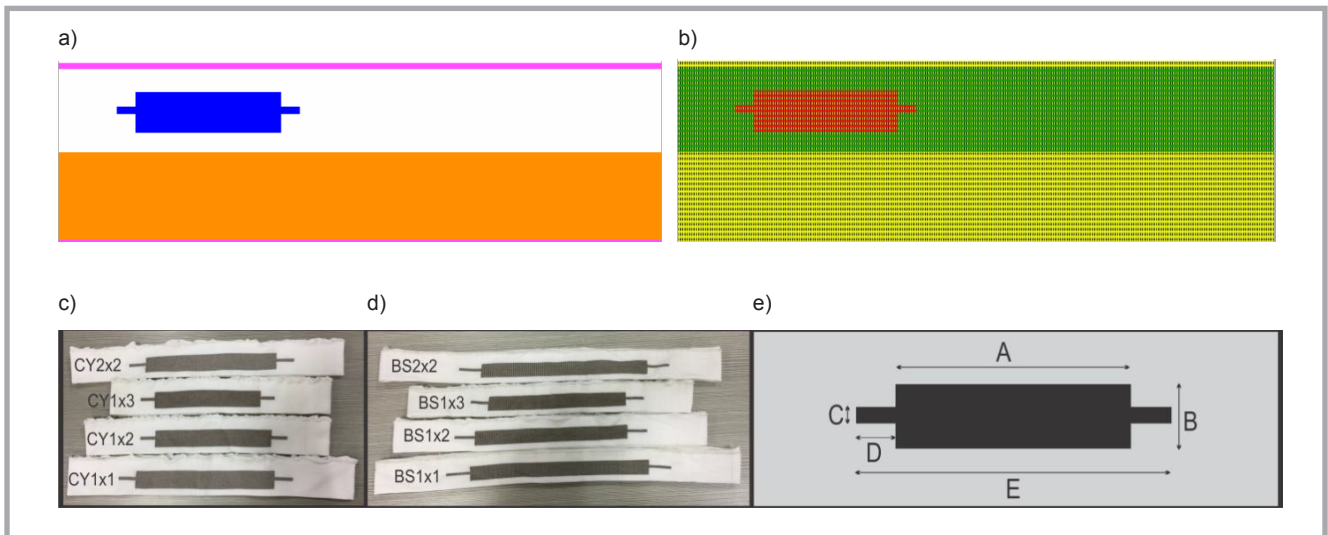


Figure 1. Design route, knitted samples and conductive surface area dimensions of samples: a) photon SDI image, b) digraph 3, quasar image, c) covered yarn samples, d) bare strand yarn samples, e) dimensions of conductive strip.

The rib fabric structure and its variations were chosen because in this envisaged product the sensor would be placed on the band, which is usually knitted using a rib structure. Rib fabric structures are characterised by raised vertical wales or ribs – one of the four basic fabric structures in weft knitting. The good shape retention character coupled with their superior elasticity has made rib structures favourable for the underwear strain sensor envisaged. Rib structures, however, vary, with numerous combinations depending on the number knits and purls within the structure. They include but are not limited to 1×1, 1×3, 2×1, 3×6 etc. These combinations have their individual characteristics and merits. Three impacts that the fabric structure proffers on the resultant fabrics were analysed, including physical or geometric and mechanical effects.

In weft knitting, machine parameters that can affect the knitted fabric are obviously dictated by the type of machine and its accompanying design software capabilities. Examples of these parameters include the machine type, gauge, diameter (circular), needle type, cam type, yarn feeding system, number of feeders, cloth take down system, cloth rolling or spreading etc. [17]. Some of these machine settings are essentially operated in their default modes and usually do not need alteration unless a special effect is desired. In this study, for example, the machine speed, air valve functions, air jet cleaning pipe functions, the yarn feed tension stitch cam setting etc., were not varied. The general settings used in

knitting common underwear were maintained and used for this study.

Seamless knitting technology usually employs the plaiting technique, where two yarns are concurrently fed to a needle. A yarn appears on the back side of the fabric in direct contact with the skin, and another on the face side of the fabric. The main yarn could be nylon, cotton, polyester or other yarn combinations, which usually appears on the face of the fabric, while the binding yarn is usually spandex or covered elastic yarn which appears on the back, and another bare elastic yarn which may be solely used for cuffs and bands to aid elastic recovery. There are many different counts and types of spandex on the market. The main ones are bare strands and single-covered, double-covered, core-spun, and core-plyed yarns. The object of spandex inclusion in the knit structure is to provide high elasticity to the resultant fabrics or apparel [18]. This elastic property is required to provide the much needed recovery that strain sensors or underwear require to guarantee extended use. This study compared the effects of bare strand (BS) or spandex and covered elastic yarns (CY) on strain sensor sensitivity and recovery.

Table 1. Count and conductive properties of yarns.

Yarn type	Linear density, tex	Resistance, Ω/cm
Silver coated yarn	4.89	77±4
Nylon covered spandex	5.56	None
Polyamide DTY	7.770	None
Bare stand spandex	2.220	None
Elastane	31.11	None

Experimental

Materials and methods

A textile structure was designed using Photon and Digraph 3 software (Dinema S.P.A., Italy). The knitting machine used was Santoni's SM8-TOP2 (Italy), Gauge number: E28, Number of feeds: 8F, Diameter 15inch, RPM:40-65r/min. 1-8Feeds. In producing CY samples, yarn finger 2 was fed with nylon covered spandex yarn, and yarn finger 5 with Polyamide DTY. Two feeds on the machine had elastane yarn which were specifically used in reinforcing cuff and band elasticity. Yarn finger 3 was thus fed with this elastane in two feeds, and plated silver conductive yarns were fed to yarn finger 8. In producing the second samples, however, yarn fingers 2 were fed with bare strand and polyamide to yarn fingers 6, respectively, with no changes at feeds 3 and 8. Properties of the yarns are shown in **Table 1**.

Sample fabrication

Fabric samples in the form of bands were designed using amalgamated software of Digraph 3 plus and photon. This study is a precursor for a prototype smart bra for measuring the breathing rate of the wearer. A band which will serve as the compo-

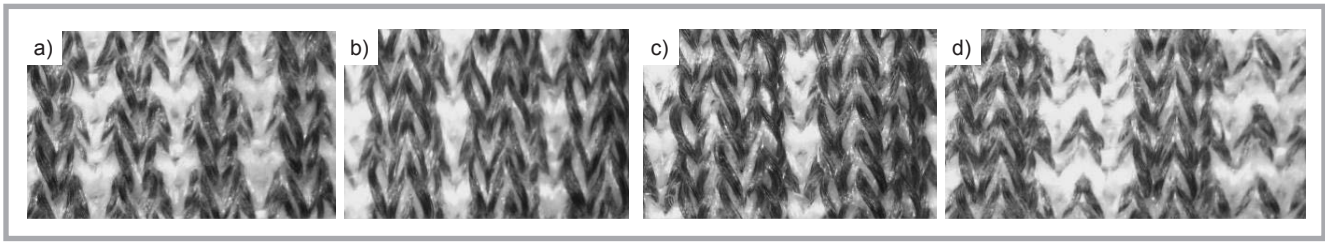


Figure 2. Micro-scale images of CY samples: a) CY1×1, b) CY1×2, c) CY1×3, d) CY2×2.

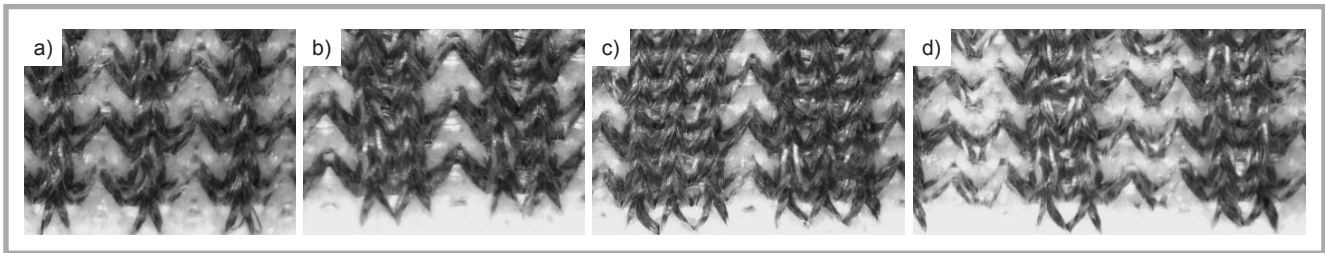


Figure 3. Micro-scale images of BS samples: a) BS1×1, b) BS1×2, c) BS1×3, d) BS2×2.

ment of the bra that will contain the strain sensor was produced. Four categories of mock rib structures were designed, namely 1×1, 1×3, 1×2 and 2×2 mock rib structures.

The designing done using a combination of Photon and Digraph 3 software (Dinema S.P.A., Italy) was subsequently transferred to the knitting machine via a USB flash disk. The Cam was set at N25, a stitch density that is usually used for undergarments. Snapshots of the designs in Photon and Digraph 3 are shown in **Figures 1.a** and **1.b**. **Figures 2** and **3** show micro-scale images of the various CY and BS knit 1c, respectively. The magnification shows clear differences in the physical properties of the structures. CY samples tend to have their conductive yarns interspersed with the covered yarns due to the inherent bulk nature of the yarn. On the other hand, the elasticity of BS yarn ensures that the conductive yarns are compactly situated within the structure. The knitted fabric

samples are also shown in **Figures 1.c** and **1.d**, with the dark part showing the conductive section. The bulk provided by CY rendered its samples thicker, with enhanced physical dimensions as compared to the BS counterparts (FC in **Table 2**). The dimensions of the conductive strip (CD) are shown in 1e, with the actual measurements in **Table 2**.

The edges of the conductive section were tapered to afford convenient clipping during testing. Preliminary physical or geometric measurements were carried out on the samples in their dry relaxed states for characterisation before subjecting them to subsequent tensile and sensitivity tests.

Physical/geometric measurements

Course and wale spacing

Course and wale spacing constitute one of the most important factors in determining the dimensional stability of knitted goods, as they are directly linked to course and wale densities, which repre-

sent changes in the stitch shape during relaxation treatments [19]. The CPC (courses per cm) and WPC (wales per cm) were measured to characterise the samples. Due to the minute nature of the loops in the structure, a 1.5 square cm window was cut out of card board, placed over the fabric, and subsequently positioned under a microscope. The WPC and CPC were counted and the figure multiplied by four to satisfy the 3×3 standard window requirement [5].

Fabric circumference (dimension)

The fabric circumference (FC) was measured using a tape measure. **Table 2** presents the physical characterisation of all the strain sensor fabric samples. The dimensions of the conductive strip (CD strip) were also measured to ascertain the total conductive surface area of all the samples. Electrical characterisation was done to ascertain the influence of fabric parameters on the resistance of the samples by measuring their resistances, also shown in **Table 2**.

Sensitivity tests

Two separate sensitivity tests were carried out, one by wearing on a human and the other via machine testing using a fabric tensile tester. The wear test enables empirical feasibility assessment of the sensor. Machine tests, on the other hand, also allow deduction of salient information that otherwise is impossible in the wear test, for example, the level of stress needed to effect deformation. It also enables lab setting simulation in the absence of human volunteers. The pie-

Table 2. Physical and electrical characterisation of fabric samples.

Samples	CPC	WPC	FC, cm	CD Strip dimensions, cm					Resistance, Ω
				A	B	C	D	E	
CY 1×1	124	104	74.2	17.8	2.2	0.4	2.3	22.5	32.75±0.05
CY 2×1	124	80	66.6	15.4	2.2	0.4	2.0	19.5	25.25±0.05
CY 1×3	124	64	60.2	14.2	2.2	0.4	1.9	18.0	25.85±0.95
CY 2×2	128	104	75	17.9	2.2	0.4	2.3	22.5	31.7±0.1
BS 1×1	208	112	68.4	18.0	1.5	0.2	2.3	22.6	14.9±0.4
BS 1×2	200	128	64	15.5	1.5	0.2	2.0	19.5	12.3±0.05
BS 1×3	200	136	58.2	14.3	1.5	0.2	1.8	17.9	11.1±0.2
BS 2×2	200	112	70.2	17.4	1.5	0.2	2.3	22.0	15.1±0.3

zoresistive responses were recorded via a custom-made test system – a pre-programmed STM32 microprocessor interfaced with a computer. The interface was programmed using C#. The sampling rate for resistance measurement was 20 samples/second. The circuitry design was optimised to ensure good signal processing output.

As tension is applied to the fabric in the course direction, the ribs which are more compact begin to pull away, resulting in the emergence of vertical grooves as the reverse loop wales (which are less compact) are exposed. Even though there is no real stretching of the yarns within the structure, the sensitivity can be directly likened to a manifestation of ohms law, as suggested by [20], where the resistance of a material is dependent on the variations in its length, resistivity and area;

$$R = \rho \frac{l}{A} \quad (1)$$

Where, R = electrical resistance, ρ = resistivity of the yarn, l = length of the conductor, and A = cross-sectional area of the conductor. The knitted loops which hitherto have been in close contact with each other tend to pull away under stress, resulting in their deformation, disengagement of the conductive contacts, and ultimately in the extension of the conductive path. The combination of the increase in the conductive path and the disruption of the intra yarn contacts are therefore responsible for the increase in resistance.

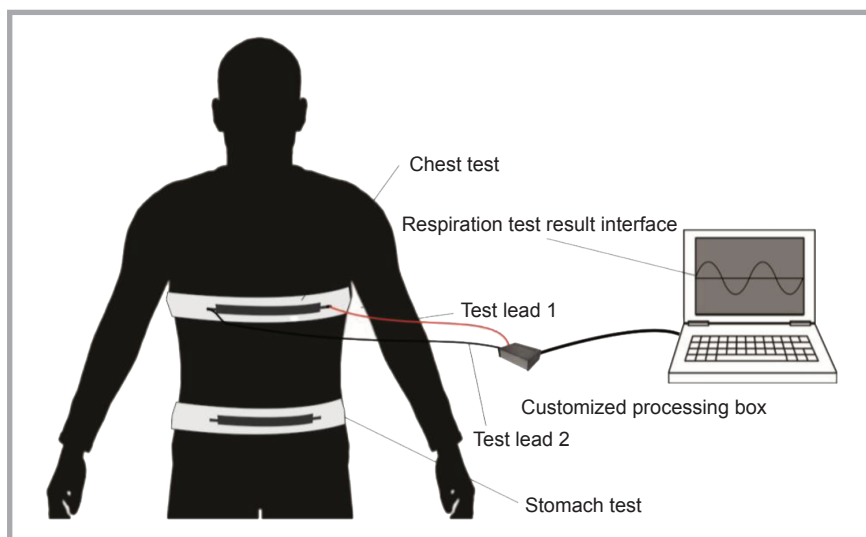


Figure 4. Set up of wear test system.

A withdrawal of the stress allows the sensor to recover its initial contacts and length. The sensitivity of the sensors is therefore governed by the ease, or otherwise, of how the structure is able to disengage from the compact conductive contacts as well as the magnitude of this disengagement due to the presence of elastic yarns within its structure.

Results and discussion

Wear test results

During breathing, the diaphragm contracts and pulls downward while the muscles between the ribs contract and pull upward. This increases the size of

the thoracic cavity and decreases the pressure inside [21]. The relaxation of all these muscles during exhalation causes the rib cage and abdomen to elastically return to their resting positions.

Experiments were carried out in which a band was worn on the chest and abdomen at separate times to test this phenomenon and to extract quantitative breathing data. Ten volunteers with no known respiratory conditions assisted in carrying out the wear tests. During the test, the wearer is required to adopt a static standing posture, as shown in Figure 4. After strapping the band around the chest or stomach, the system is switched on, and the volunteer

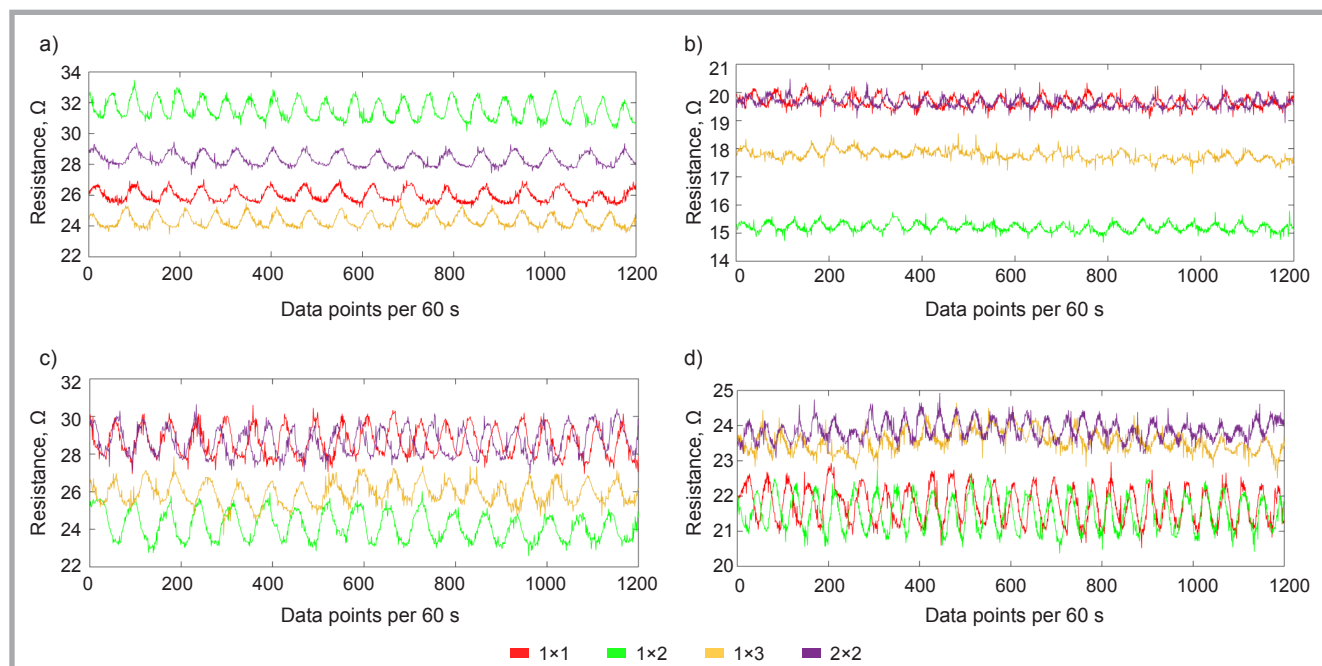


Figure 5. Single chest and stomach breathing cycle patterns of samples: a) chest breath pattern of CY Samples, b) chest breath pattern of BS samples, c) stomach breath pattern of CY samples, d) stomach breath pattern of BS samples.

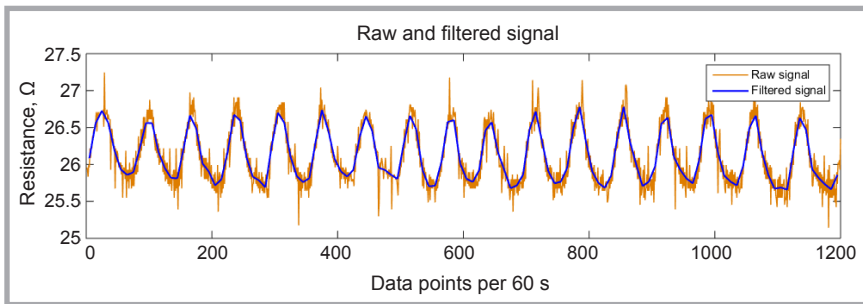


Figure 6. Breathing pattern before and after filtering.

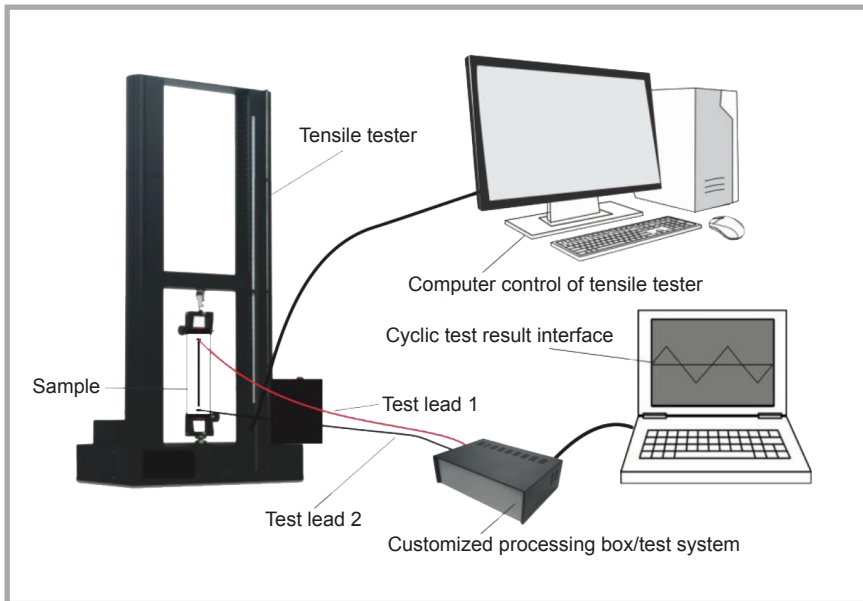


Figure 7. Machine test set up.

is encouraged to breathe as normal as possible with the face facing away from the screen to minimise anxiety.

The expansion of the chest and or the abdomen caused the resistance of the sensor to increase and to decrease upon chest or abdominal contraction, or vice versa. Figure 5 shows the pattern of a single chest and abdominal breathing cycle of both covered bare strand yarn samples, i.e. exhale/inhale cycles over a period of 60 seconds.

There are variations in amplitudes for individual breathing cycles. However, the frequency of breathing for each sensor appears uniform as the peaks are evenly spaced on the time scale.

Peaks for stomach samples are higher than for their chest counterparts, which is normal as the abdominal response to breathing has been confirmed to be more pronounced than in the case of the chest [22, 23]. Also, as can be seen, the patterns involving different elastic yarn

samples have slight differences in wavelengths. The shorter wavelengths of BS samples are an indication of their faster recovery after stretching within a breathing cycle. The CY samples had slightly longer wavelengths due to slow recovery after stretching within a breathing cycle. The bulk characteristic of CY, shown in Figure 2, is responsible for the slow recovery. The influence of the rib structure type on sensor test results is minimal, as shown in Figure 5.

There is no clear deviation in the wavelengths of both chest and stomach CY samples due to differences in the knit structure. Unlike the machine test signals, the breathing signals are fraught with some noise, due to the band being exposed to pretension when worn. The combination of the wearing pretension, breathing response tension and other body movements is responsible for the noise. An average filter was applied to filter out the noise while preserving the original profile of the sine wave as much as possible, as shown in Figure 6.

Wearing test results for BS were comparatively inferior to those covered yarn samples. This is because spandex knitted samples tended to be tighter due to the impact of the highly elastic yarns (Figure 3), and therefore need a larger range of fabric deformation to be responsive. Chest test results are shown in Figure 5.b; where minute deformation delivered poor response; however, abdominal breathing, which imposes much more stress, resulted in much more improved piezoresistive response (Figure 5.d).

Machine test results

Machine sensitivity tests were carried out using a Ningbo Kewei multi-functional electronic fabric strength tester. The samples were subjected to cyclic tension to simulate oscillatory breathing situations. Using alligator clips, the samples were connected to a customised test system interfaced with a computer, the scheme of which is shown in Figure 7. The fabric tester was also controlled by a computer. There was 15 load – unload cycles of deformation at a fixed strain level of 10% and tensile speed of 900 m/s.

Figure 8 shows the piezoresistive response of both covered yarn and bare strand knitted samples under machine cyclic tension tests. As seen in Figure 7, the signals tend to have very similar wavelengths, but with slight variations in amplitudes. This can be attributed to the viscoelastic behaviour of the elastic materials absorbing elastic energy in the cycles.

The stress strain results of a single stress cycle are presented in Figures 8.b, 8.d for all yarn samples. 2×2 structure samples in this category tend to use more force in the deformation, followed by 1×3, 1×2 and 1×1 in that order. 1×1 proved to be the most extensible, which is clearly shown in the stress strain curves in Figures 8.b and 8.d. A comparison between the stress strain curves of the two yarn samples indicates that CY samples require more force to undergo deformation. The characteristic minimal force for the deformation of BS samples can be attributed to the spandex yarn content which makes them less dense. Therefore the lighter they are, the less force required to deform them.

In order to ascertain the sensitivity of the sensors, computation of what we describe as the average peak value (APV) was done for each group of samples and compared. The APVs were computed

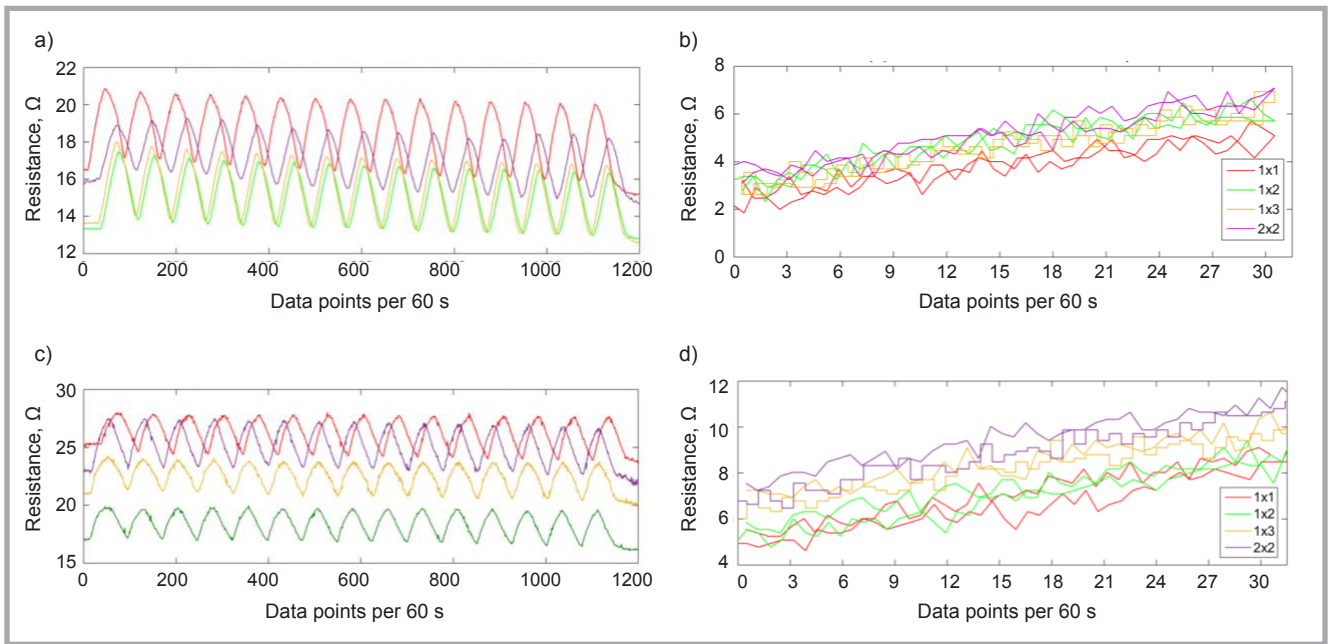


Figure 8. Cyclic test results and stress strain curves of CY and BS samples: a) cyclic tensile test results of BS samples, b) stress strain curve of BS samples, c) cyclic tensile test results of CY samples, d) stress strain curve of BS samples.

by finding the average peak resistance change per cycle of the test, followed by subtraction and division with the initial resistance. This resultant figure gives a good estimation of the average magnitude of change in resistance per cycle test. **Figure 9** shows the APVs of all three test categories. The average peak value results for machine tests establish that BS yarn knitted samples subjected to machine tensile tests performed better than their CY counterparts.

This is because the machine test produced a larger force to deformation; a range where the knit structure is able to have ample separation of the compact conductive loops. The increase in the conductive path is thus significant, hence the higher sensitivity. The wear test results showed a higher APV for CY samples compared to BS samples due to the ability of those

structures to attain longer paths under low deformation.

The two main production parameters – yarn type and knit structure had clear physical and electrical effects on the knitted samples. The 2×2 mock rib structure had a larger diameter size, followed by 1×1, 1×2 and 1×3 in that order. Samples 1×1 and 1×2 had the highest levels of resistance, which can be attributed to their comparatively longer dimensions, and thus to the conductive paths.

The absence of bulk provided by the covered yarn in spandex (BS) samples resulted in reduced physical dimensions. Their compact nature is reflected in their micro-images, shown in **Figure 3**, and their large stitch density. Generally bare strand yarn samples had lower levels of resistance. Even though the conduc-

tive strips of the bare strand samples are close to their covered yarn counterparts in terms of dimensions, their rather compact structure, devoid of bulk, facilitated good conduction, accounting for their lower resistances.

Machine tensile test results showed good results with marginal peak fluctuations in signals. However, variation existed in the peaks of the signals from the chest and abdominal tests in somewhat pronounced forms. This may be partly as a result of respiratory variation, which is sometimes considered normal [24, 25]. However, many other factors have also been attributed to this occurrence. Considering the fact that this study is not geared towards qualitative breathing pattern analysis, these are issues that need further investigation if breathing sensors are to be recommended for clinical applications. However,

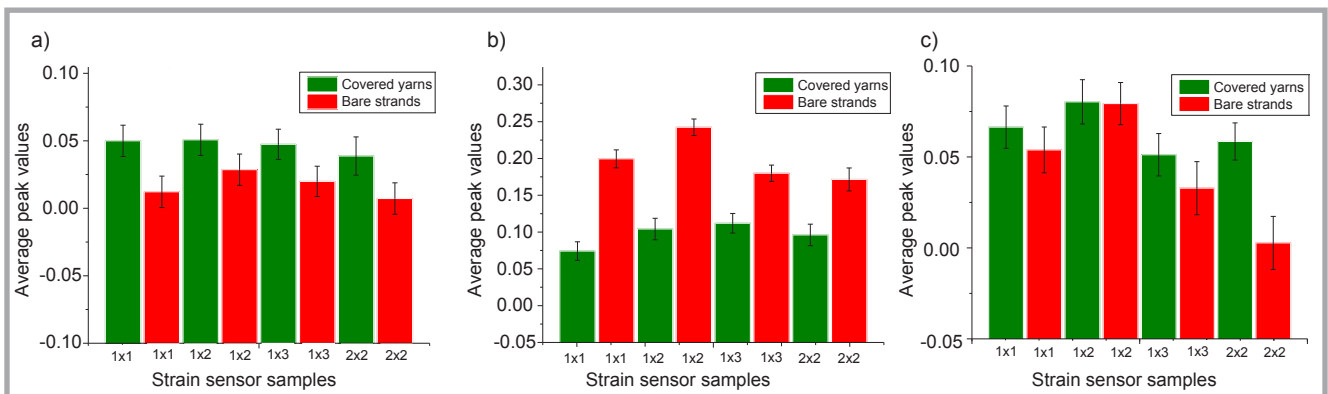


Figure 9. Average peak values of samples: a) for chest test results, b) for machine test results, c) stomach test results.

it is also worthy to note that the signals obtained compare favourably with other wear tests cited in literature [26].

Dimensional stability

Fatigue is a progressive, localised, permanent structural change that occurs in materials that are subjected to cyclic stress and strains. Fatigue in textiles is usually measured in terms of its bagging effect. However, with regards to this experiment, we resorted to possible dimensional changes in samples to predict the possible fatigue behaviour of sensors. This is because cuffs and bands embedded with elastic yarns generally enjoy immunity from dimensional distortions as elastic yarns need over 200% extension to break [27].

After several wear and tensile tests, no visible dimensional changes were observed in the samples, and diameter measurements retaken showed no differences compared to the ones made prior to the experiments. This is due to the generally good shape retention characteristics of spandex embedded fabrics [28] and also to the rather minimal percent of tension imparted to the samples during tensile tests. However, slipping the bands on and taking them off during wear tests imposed much more stress; but the samples recovered quickly after being taken off.

Repeatability/stability/aging

Repeatability is the ability of a sensor to consistently reproduce the same output signal for repeated measurements of the same value over a specified period. In the short term, it is called stability, while it is called aging in the long term. In this study, sensor performance after 1, 10 and 50 days was tested to ascertain the sensor's stability after prolonged use. After about 50 days of testing, there was no noticeable deviation in sensor response, which indicates good sensor stability of the samples. Cronbach's alpha coefficient was thus used to measure the aging reliability or repeatability of machine test results for day 1, 10 and 50. High reliability was found for most samples with Cronbach's alpha computations yielding $\alpha = 0.87$ for 1×2 CY, $\alpha = 0.97$ for 1×3 CY, $\alpha = 0.97$ for 2×2 CY, $\alpha = 0.83$ for 1×1 BS, $\alpha = 0.89$ for 1×2 BS, $\alpha = 0.76$ for 1×3 BS, and $\alpha = 0.98$ for 2×2 BS respectively. However 1×1 CY had lower alpha; $\alpha = 0.65$. Cronbach's alpha is utilized as a measurement index of reliability for

a test or instrument which could be obtained from a single experiment given the practical difficulties. Alpha values greater than 0.70 is an indication of high stability of results.

Conclusions

On a whole, all four knit structures delivered satisfactory results, making any of them fit for use as strain sensors for breathing mensuration. However, in selecting any of the knit structures, sizing requirements should be considered as different structures resulted in different sizes of garments. 1×3 rib delivers the smallest circumference, followed by 1×2 , 2×2 and 1×1 rib structures in that order.

The influence of elastic yarn type also influenced, to a large extent, the resistance of the conductive fabrics. A comparison of the average peak values in **Figures 8.b** and **8.c** indicate that bare strand elastic yarn samples had significantly reduced electrical resistance change under minimal deformation compared to covered yarn samples. However, under higher deformation, change in resistance is rather significant (**Figure 9.a**). BS samples also require comparatively less force to deform under tensile stress. Even though CY samples require higher force to deform the structure due to bulk, the sensitivity under a small range of deformation is impressive. The high resistance change to minimal stress range behaviour exhibited by CY samples makes them more favourable for application as breathing detection sensors due to the superior results attained in wear tests.

As demonstrated, the strain sensors fabricated and used in a wearable environment provided useful descriptive information about the breathing frequency of the wearer; however, further characterisation tests are required to assess the possibility of accessing other breathing parameters before prescription for clinical applications. Further studies, therefore, need to be geared towards sensor characterisation and testing in different user conditions and the results compared with standard clinical instruments

Acknowledgements

The authors acknowledge the financial support from the Science Foundation of Jiangsu Province (BK20151129); Fundamental Research Funds for the Central Universities (JUSRP51727A).

Conflicts of interest

The authors declare no conflict of interest.

References

1. Wijesiriwardana R. Inductive fiber-meshed strain and displacement transducers for respiratory measuring systems and motion capturing systems. *IEEE Sensors Journal* 2006; 6(3): 571-9.
2. Waqas Qureshi, Li Guo, Joel Peterson, Adib Kalantar Mehrjerdi, Skrifvars M. *Knitted wearable stretch sensor for breathing monitoring application*. Ambience; Borås, Sweden, 2011: 1-5.
3. Asli A, Ozgur A, Muhammad DH, Anura F, Prasad P. Piezofilm yarn sensor-integrated knitted fabric for healthcare applications. *Journal of Industrial Textiles* 2016; 47(4): 505-21.
4. Grillet A, Kinet D, Witt J, Schukar M, Krebber K, Pirotte F, et al. Optical Fiber Sensors Embedded Into Medical Textiles for Healthcare Monitoring. *IEEE Sensors Journal* 2008; 8(7): 1215-22.
5. Frutiger A, Muth JT, Vogt DM, Menguc Y, Campo A, Valentine AD, et al. Capacitive Soft Strain Sensors via Multicore-Shell Fiber Printing. *Advanced Materials* 2015; 27(15): 2440-6.
6. Ehrmann A, Heimlich F, Brucken A, Weber M, Haug R. Suitability of Knitted Fabrics as Elongation Sensors Subject to Structure, Stitch Dimension and Elongation Direction. *Textile Research Journal* 2014; 84(18): 1-16.
7. Gal Y, inventor; adidas AG (Herzogenaurach, DE), assignee. Sensors for inductive plethysmographic monitoring applications and apparel using same. US patent 8777868. 2014.
8. Zhou J, Gu Y, Fei P, Mai W, Gao Y, Yang R, et al. Flexible Piezotronic Strain Sensor. *Nano Letters* 2008; 8(9): 3035-40.
9. Hoffmann K. *An Introduction to Stress Analysis and Transducer Design using Strain Gauges*. HBM Test and Measurement. hbm.com: Hottinger Baldwin Messtechnik GmbH; 2016, p. 10-1.
10. Raji RK, Miao X, Boakye A. Electrical Conductivity in Textile Fibers and Yarns-Review. *AATCC Journal of Research* 2017; 4(3): 8-21.
11. Atalay O, Kennon W, Husain M. Textile-Based Weft Knitted Strain Sensors: Effect of Fabric Parameters on Sensor Properties. *Sensors* 2013; 13(8): 11114-27.
12. Ozgur A, Kennon WR. Knitted Strain Sensors: Impact of Design Parameters on Sensing Properties. *Sensors* 2014; 14(3): 4712-30.
13. Kaldor J, James D, Marschner S. Simulating knitted cloth at the yarn level. *ACM Transactions on Graphics* 2008; 27(3): 65.
14. Fatkić E, Geršak J, Ujević D. Influence of Knitting Parameters on the Mechanical Properties of Plain Jersey Weft Knit

- ted Fabrics. *FIBRES & TEXTILES in Eastern Europe* 2011; 19, 5(88): 87-91.
15. Xie J, Long H. Equivalent resistance calculation of knitting sensor under strip bi-axial elongation. *Sensors and Actuators A-physical* 2014; 220: 118-25.
 16. Hu J, Lu J. *Recent developments in elastic fibers and yarns for sportswear* In: Shishoo R, editor. *Textiles for Sportswear*: Woodhead Publishing; 2015. p. 53-76.
 17. Eltahan EAE, Sultan M, Mito A-B. Determination of loop length, tightness factor and porosity of single jersey knitted fabric. *Alexandria Engineering Journal* 2016; 55(2): 851-6.
 18. Marmarali AB. Dimensional and Physical Properties of Cotton/Spandex Single Jersey Fabrics. *Textile Research Journal* 2003; 73(1): 11-4.
 19. Herath CN, Kang BC. Dimensional Stability of Core Spun Cotton/Spandex Single Jersey Fabrics under Relaxation. *Textile Research Journal* 2008; 78(3): 209-16.
 20. Atalay O, Tuncay A, Husain MD, Kennon WR. Comparative study of the weft-knitted strain sensors. *Journal of Industrial Textiles* 2015; 46(5): 1212-40.
 21. Nozoe M, Mase K, Takashima S, Matsu-shita K, Kouyama Y, Hashizume H, et al. Measurements of chest wall volume variation during tidal breathing in the supine and lateral positions in healthy subjects. *Respiratory Physiology & Neurobiology* 2014; 193 (Supplement C): 38-42.
 22. Kaneko H, Horie J. Breathing movements of the chest and abdominal wall in healthy subjects. *Respiratory Care* 2012; 57(9): 1442-51.
 23. Mohan V, Dzulkifli NH, Justine M, Haron R, H LJ, Rathinam C. Intrarater Reliability of Chest Expansion using Cloth Tape Measure Technique. *Bangladesh Journal of Medical Science* 2012; 11(4): 307-11.
 24. Hammer J, Newth CJL. Assessment of thoraco-abdominal asynchrony. *Paediatric Respiratory Reviews* 2009; 10(2): 75-80.
 25. Fadel PJ, Barman SM, Phillips SW, Gebber GL. Fractal fluctuations in human respiration. *Journal of Applied Physiology* 2004; 97(6): 2056-64.
 26. Atalay O, Kennon WR, Demirok E. Weft-Knitted Strain Sensor for Monitoring Respiratory Rate and Its Electro-Mechanical Modeling. *IEEE Sensors Journal* 2015; 15(1): 110-22.
 27. Senthilkumar MN. A. Elastane fabrics – A tool for stretch applications in sports. *Indian Journal of Fibre and Textile Research* 2011; 36(3): 300-7.
 28. Mukhopadhyay A, Sharma IC, Mohanty A. Impact of lycra filament on extension and recovery characteristics of cotton knitted fabric. *Indian Journal of Fibre & Textile Research*. 2003; 28(4): 423-30.

Received 14.03.2018 Reviewed 25.06.2018



IBWCh

Institute of Biopolymers and Chemical Fibres

*FIBRES & TEXTILES
in Eastern Europe
reaches all corners
of the world!*

*It pays
to advertise your products
and services in our magazine!
We'll gladly
assist you in placing
your ads.*

FIBRES & TEXTILES in Eastern Europe

ul. Skłodowskiej-Curie 19/27
90-570 Łódź, Poland

Tel.: (48-42) 638-03-00, 637-65-10

Fax: (48-42) 637-65-01

e-mail:

ibwch@ibwch.lodz.pl infor@ibwch.lodz.pl

Tel.: (48-42) 638-03-14, 638-03-63

Internet:

<http://www.fibtex.lodz.pl>